

# Double Laser Annealing of Implanted Silicon by using Laser Pulse Offsets

V. Gonda, J. Slabbekoorn, and L.K. Nanver

**Abstract**— Double-pulsed high-power excimer laser annealing is investigated for use as a means of implanted dopant activation. The laser setup incorporates two lasers that allow double pulse laser annealing with pulse offsets much smaller than the repetition of the individual XeCl excimer lasers. In this configuration, the pulse offset can be fine tuned. Sheet resistances are measured and thermal simulations are conducted to study temperature profiles. Results show, that the total laser energy needed for a complete activation increases with the pulse separation. By using non-equal pulse energies, complete separation occurs earlier and pre-heating arrangement is favorable to post-heating. In this way the thermal budget can be tuned with more freedom.

**Index Terms**—double laser annealing, non-equal pulses.

## I. INTRODUCTION

ULTRA-SHALLOW implantations can be activated with very low thermal budget by excimer laser annealing. We have demonstrated near-ideal implanted and excimer laser annealed p- and n-type diodes with single shot annealing [1]. However, due to the very low thermal budget, significant residual implantation damage can remain below the laser melted and regrown region causing deactivation in the underlying layers and junction leakage [2]. Increasing the thermal budget is beneficial for defect annealing [3, 4] while maintaining the heat affected zone shallow. The thermal budget can be increased by increasing the laser pulse length. By this, the heat diffusion length also increases; the upper limit is the thermal limitation of the underlying layer.

While most laser setups consist of one laser, some groups have investigated double laser processing with excimer and Ar<sup>+</sup> laser [5] or two solid state lasers [6]. A double laser setup has recently been custom built by Exitech for DIMES. It incorporates two Lambda Physik LPX 210 laser sources using XeCl with wavelength of 308 nm. The native pulse duration is 25 ns at full width at half maximum. The two laser operation gives the opportunity to extend the pulse length by introducing a pulse offset between the two laser pulses in equal energy density mode [7]. Short pulse offsets may result in non-uniformities by the time jitter between the firing of the lasers.

In this paper, we demonstrate double laser annealing with

variable pulse offsets using non-equal pulses by measuring sheet resistances of the laser annealed implantations. At zero offset, the pulses are completely overlapping, and therefore providing the largest power. As the offset increased and peak power drops, the total energy density remains unchanged and therefore the surface temperature drops. In this regime, the effective pulse duration is longer. When the laser pulses are separated further, the generated heat pulses separate, the effective energy density reduces and is ultimately equal to the largest pulse's energy. The temperature drop can be compensated by increasing the laser energy density and/or the substrate temperature. Spot-to-spot uniformity improves with increasing pulse separation. In practice, the longer pulses have a beneficial effect on reducing defect concentrations below the amorphous/crystalline interface [6]. By using dissimilar pulse amplitudes, pre- and post-heating can be realized. The optimal pulse separation and amplitude ratio can be found for a given thermal limitation at a spot-to-spot uniformity tolerance.

## II. EXPERIMENTAL PROCEDURES

A schematic of the laser crystallization setup is shown in Fig. 1. It consists of two Lambda Physik LPX 210 XeCl excimer laser sources with a wavelength of 308 nm, pulse duration of 25 ns (full width at half maximum), which are triggered by the pulse generator. Different pulse offsets can be realized by the pulse generator settings, the jitter between the laser pulses at  $1\sigma$  is 4 ns. The energy densities are set with the attenuators after which the laser beams are combined. A homogenizer was used to produce a flat-top intensity profile with a 7% energy variation across a 10 mm<sup>2</sup> area. On each wafer the laser energy densities are varied in columns.

The starting material for the samples is (100) p-type silicon wafers. The n<sup>+</sup> implanted regions to be laser annealed are formed by a 15 keV,  $4 \times 10^{15}$  cm<sup>-2</sup> As<sup>+</sup> implantation. This implantation gives an amorphous depth around 50 nm, and when the implant is fully activated by the laser anneal, the sheet resistance drops below 300 ohm/sq.

The laser annealing after the implantation was performed in vacuum, with a laser pulse overlap of 66%. The laser pulse ratio was chosen as 1:2. The pulse offsets are set for different wafers at 0, 100, and 200 ns. An example of the pulse shapes for increasing offsets are shown in Fig. 2. The laser anneals were performed in vacuum, the substrate was kept at room temperature. The sheet resistance of each wafer was measured by 4 point sheet resistance mapping over the wafer with the

Manuscript received October 1, 2007. This work was supported by NXP.

All authors are with the Delft University of Technology, DIMES-ECTM, Feldmannweg 17, POB 5053, 2600 GB Delft, The Netherlands (phone: +31 15 27 88837, fax: +31 15 262 2163, e-mail: v.gonda@dimes.tudelft.nl).

### III. THERMAL SIMULATIONS

A 1-D thermal simulation was used to estimate temperature profiles in the silicon wafer at double laser irradiation.

The transient heat transfer equation is formulated as

$$\rho c_p(T) \frac{\partial T}{\partial t} = \frac{\partial}{\partial x} \left( k(T) \frac{\partial T}{\partial x} \right) + Q(t) \quad (1)$$

where  $\rho$  is the mass density,  $c_p$  the specific heat capacity,  $k$  the heat conductivity,  $T$  the absolute temperature,  $t$  the time. The  $Q$  is the heat generated in the silicon from the laser pulse. It is given by

$$Q(t) = (1 - R)I(t) \quad (2)$$

where  $R$  is the reflectivity of the surface, and  $I$  the intensity of the laser pulse.

The boundary conditions that are applied in the numerical simulations are given by setting the surface for inward heat flux during the laser irradiation as in Eq. 2, otherwise insulated:

$$\left. \frac{\partial T}{\partial x} \right|_{x=0} = 0, \quad (3)$$

and at the substrate beyond the zone affected by the laser heating the temperature is set to constant ambient temperature:

$$T(x_{\max}) = 300K. \quad (4)$$

A 1-D portion of silicon to a depth of  $10 \mu\text{m}$  was simulated with a dense mesh being used close to the surface. The c-Si material density was  $\rho = 2.33 \text{ g/cm}^3$ . Temperature dependent thermal properties are shown in Fig. 3. for c-Si were obtained from literature [3, 8]:

$$k(T) = 0.235 + 4.45 \exp(-T(K)/247) \quad (5)$$

$$c_p(T) = 0.81 + 1.3 \cdot 10^{-4} T - 1.26 \cdot 10^{-4} T^{-2} \quad (6)$$

The laser pulse shape was approximated as a smooth trapezoidal-like shape with a 10 ns rise time, 10 ns hold time and 30 ns fall time, where the pulse full width at half maximum was 25 ns.

The pulse energy ratio was set to 1:2, therefore 1000 mJ/cm<sup>2</sup> total energy density was a result of a 666 mJ/cm<sup>2</sup> large pulse and a 333 mJ/cm<sup>2</sup> small pulse, the pulse heat was calculated for reflectivity  $R = 0.7$ , and incorporated as a surface heating.

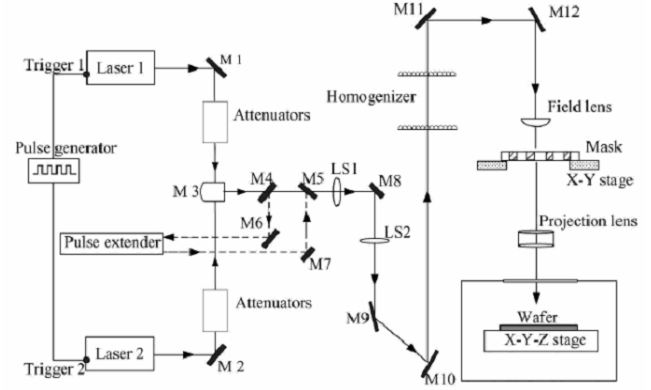


Fig. 1. Schematic of the double laser annealing setup.

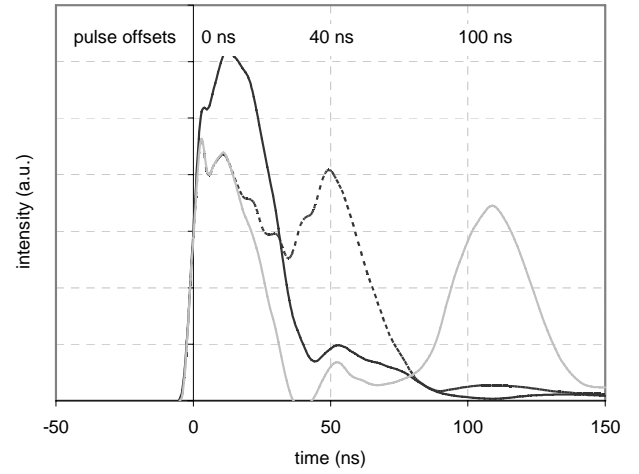


Fig. 2. Pulse shapes as a result of combining two equal laser pulses with offsets of 0, 40 and 100 ns.

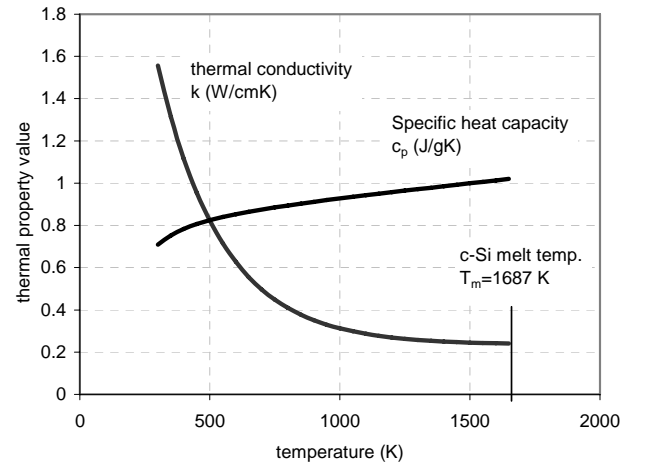


Fig. 3. Temperature dependent thermal conductivity and specific heat capacity for c-Si used in the numerical simulations [3, 8].

## A. Simulation results

Temperature history is shown for the irradiated silicon surface by double laser annealing with various pulse offsets (Fig. 4). For the simple simulated case of irradiating c-Si, the heat generated from a single laser pulse can be superimposed, to approximate the heating effect. Therefore, as the temperature decays from the first pulse, it gives lower and lower initial temperature for the second pulse, hence a lower overall temperature can result. In case of the pre-heating pulse arrangement, the small pulse is first (pulse order 1:2), than the maximum temperature is always reached by the second (large) pulse. In case of a post-heating arrangement, the peak temperature is reached by the first (large) pulse at large pulse offsets.

The absolute temperature profile would be different if the thin amorphous implanted layer would have been considered: a-Si has lower absorption for the lasing wavelength, as well as much lower thermal conductivity, somewhat higher heat capacity, and a lower melting temperature. All in all, this would result in a faster heating up. Considering phase transformation at melting, latent heat can act as a buffer for the heat. As melting reaches the amorphous/crystalline interface, the difference in melting temperature limits the process, and the melting only progresses further if the temperature reaches the melting point of c-Si. The regrown Si properties are very much dependent on the process of cooling by which the heat injected into the silicon surface is conducted away by the bulk substrate.

Although a basic thermal model was used in the simulation, it still gives a good estimate of the total heating, in the view of the fact that the cooling properties are very important and the thermal budget is otherwise correct. However, thermal losses due to radiation and ablative processes can cause deviations in the total heating/cooling times.

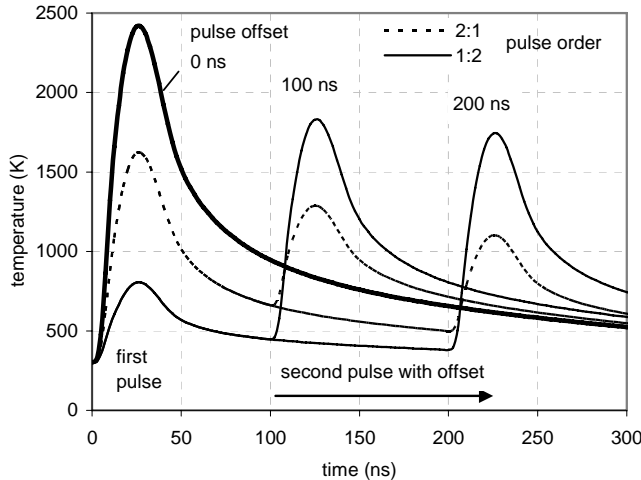


Fig. 4. Surface temperature history in double pulse laser annealing with total energy of  $1000 \text{ mJ/cm}^2$  (large pulse:  $667 \text{ mJ/cm}^2$ , small pulse  $333 \text{ mJ/cm}^2$ , and pulse offsets from 0, 100, and 200 ns.

## B. Wafer samples

Figure 5 shows the measured sheet resistance values for samples laser annealed with pulse offsets of 0 and 200 ns in a pre-heating pulse arrangement (small pulse followed by a large pulse, with energy ratio 1:2). In general, increasing total laser energy density is needed with increasing pulse offsets in order to achieve a certain melt depth/ sheet resistance. The effective laser energy is in between the total and the largest pulse energy:

$$E_{total} = E_1 + E_2 \geq E_{eff} \geq \max(E_1, E_2). \quad (7)$$

The curves in Fig. 5 show the extremities: at 0 ns offset the two laser pulses are completely overlapped, resulting in one pulse with the largest possible peak power and the effective laser energy equals the total energy density. At 200 ns offset, however, not only the laser pulses are separated, but also the generated heat pulses are separated. This happens at smaller offsets at non-equal pulse energies than at equal pulse energies, where complete separation occurred at 400 ns for the same implantation [7].

In the present case, the second (large) pulse is responsible for the activation process opposed to the equal-pulse or post-heating arrangement. The first (small) pulse has so low energy (Fig 5.), that it can not initiate phase changes in the amorphous layer, and its heating effect vanishes at already 200 ns offsets. Melting of a thin layer of the a-Si can start at energies of  $500 \text{ mJ/cm}^2$ , but then the second pulse is so high that the initial effect is negligible.

As the small pulse has negligible effect, the effective laser energy density equals to the energy density of the large laser pulse, e.g. to reach  $400 \text{ ohm/sq}$  activation, at 0 offset both pulses contribute at a total of  $800 \text{ mJ/cm}^2$ , while at 200 ns pulse offset this sheet resistance is reached at  $1200 \text{ mJ/cm}^2$  total energy density, of which only the large pulse is effective, that is exactly  $800 \text{ mJ/cm}^2$ .

Figure 6 shows a comparison of the different pulse arrangement (equal pulses: 1:1, large pulse first: 2:1, small pulse first: 1:2) at 100 ns pulse offsets. Apparently, this offset falls into the small offset range, where the heat pulses generated from the laser pulses are not separated yet, therefore both laser pulses contribute to the effective laser energy. In other words, the resulting sheet resistances can not be reached with a single pulse set to the largest contributing energy.

At 1:1 and 2:1 cases the first pulse reaches melting and latent heat keeps the melting pool, then the second pulse contributes with more heat. The effect of the first pulse is important, in 2:1 the first pulse is larger than in 1:1, therefore the resulting sheet resistance is smaller. Melting starts at about  $500 \text{ mJ/cm}^2$ . Solidification has not started after 100 ns. In the simulation results, this regime is not captured: amorphous heats faster, liquid keeps latent heat.

In case of 1:2 pulse order the first pulse is so small, that it can not melt, however, a-Si keeps heat longer, and the second pulse starts at elevated temperature and melts, a similar

situation like laser annealing with substrate heating in [7].

Sheet resistance equals out at high enough laser energies (total energy > 1300 mJ/cm<sup>2</sup>) for 1:2 and 2:1, because for the former case, the small first pulse energies become large enough for melting

Table I summarizes the results for the sheet resistances at 100 ns offset at 1000 mJ/cm<sup>2</sup> total energy. The increase in the peak temperatures extracted from the simulations corresponds to the decrease of the sheet resistance.

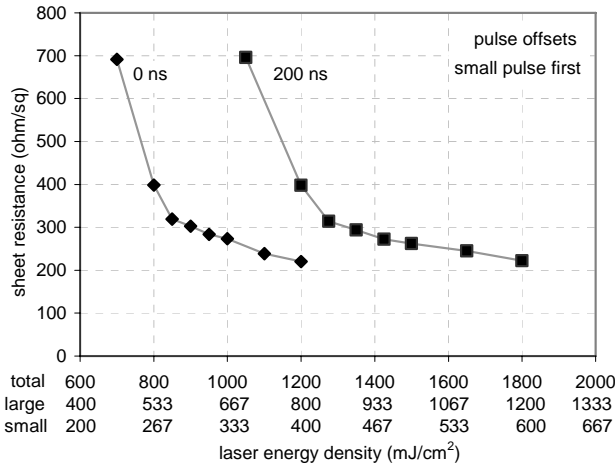


Fig. 5. Sheet resistance of a double laser annealed As<sup>+</sup> 15 keV, 5x10<sup>14</sup> /cm<sup>2</sup> implant with ELA at different pulse offsets in a pre-heating pulse arrangement. Laser energy densities are shown for the small and the large pulse as well as their sum (total) on the horizontal axis.

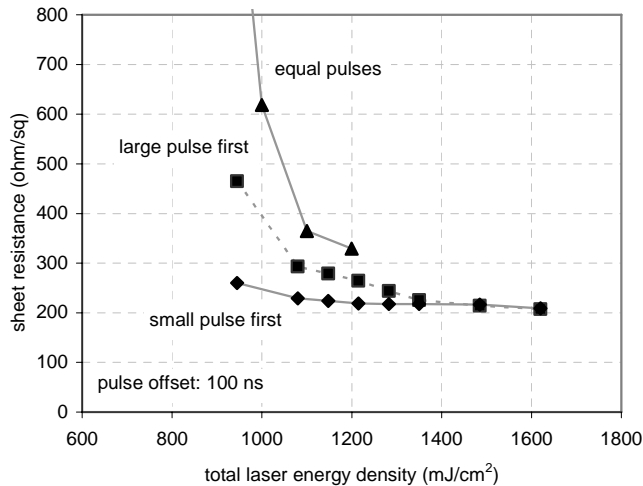


Fig. 6. Sheet resistance of a double laser annealed As<sup>+</sup> 15 keV, 5x10<sup>14</sup> /cm<sup>2</sup> implant with 100 ns offset at different pulse energy orders of 1:1, 2:1, 1:2.

Table I. Sheet resistance measured for a total laser energy of 1000 mJ/cm<sup>2</sup> at 100 ns pulse offsets. Simulated peak temperatures can occur at the first or the second pulse.

pulse E ratio	R <sub>s</sub> (ohm/sq)	T <sub>max</sub> (°C)	T <sub>max</sub> @ pulse
500:500	618	1550	2
667:333	400	1620	1
333:667	250	1830	2

## V. CONCLUSION

It has been demonstrated that in the use of double-pulse laser annealing of implanted silicon regions, the pulse offset is an important parameter for the total amount and reproducibility of the heat transfer to the Si. As a general result, it is shown that with increasing the pulse separation higher laser energy is needed to fully activate implantations. This is a result of the fact the temperature rise due to the second pulse superposes on the heat profile generated by the first pulse, thus a higher energy of the individual pulses is needed to achieve the desired heat transfer as the pulse offset is increased. The use of non-equal energies makes the complete separation offset smaller. The use of pre- or post heating arrangements has different effects on the sheet resistances in the small offset regime: the pre-heating results in lower sheet resistances as the small first pulse does not induce melting, therefore the second pulse does not hit liquid Si.

## REFERENCES

- [1] V. Gonda, A. Burtsev, T.L.M. Scholtes, and L.K. Nanver, "Near-ideal implanted shallow-junction diode formation by excimer laser annealing," in Proc. IEEE-RTP, Vol. 13, pp. 93-100, 2005
- [2] V. Gonda, S. Liu, T.L.M. Scholtes, and L.K. Nanver, "Electrical characterization of residual implantation-induced defects in the vicinity of laser-annealed implanted ultrashallow junctions," in Doping Engineering for Device Fabrication, edited by B.J. Pawlak, S.B. Felch, K.S. Jones, M. Hane (Mater. Res. Soc. Symp. Proc. 912, Warrendale, PA), 2006
- [3] A. Matsuno, K. Kagawa, Y. Niwatsukino, T. Nire, K. Shibahara, "Pulse duration effects on laser anneal shallow junction," in Proc. ECS-ISTC, Vol. 2002-17, pp. 148-156, 2002.
- [4] J. Venturini, "Long pulse laser thermal processing: annealing duration trade-off for next generation semiconductors hot processes," in Proc. IEEE-RTP, Vol. 13, pp. 111-117, 2005.
- [5] M. Lee, S. Moon, M. Hatano, C.P. Grigoropoulos, "Ultra-large lateral grain growth by double laser recrystallization of a-Si films," in Appl. Phys. A 73, 317-322, 2001.
- [6] T. J. Kudo, "Double-pulsed laser annealing technologies and related applications," in Proc IEEE-RTP, Vol. 14, pp. 21-29, 2006.
- [7] V. Gonda, J. Slabbekoorn, L.K. Nanver, "Silicon laser annealing by two-pulse laser system with variable pulse offsets", in Proc. IEEE-RTP, Vol 15, 2007.
- [8] S. de Unamuno, E. Fogarassy, "A thermal description of the melting of c- and a-Silicon under pulsed excimer lasers," in Appl. Surf. Sci. 36, pp. 1-11, 1989.
- [9] E. Fogarassy, C. Fuchs, S. de Unamuno, P. Siffert, "Excimer laser induced melting of heavily doped silicon: a contribution to the optimization of the laser doping process," in Appl. Surf. Sci. 43, pp. 316-320, 1989.